Non-Muscle Actin Filament Elongation from Complexes of Profilin with Nucleotide-Free Actin and Divalent Cation-Free ATP−Actin†

Henry J. Kinosian,*,‡,§ Lynn A. Selden,§ Lewis C. Gershman,§,|| and James E. Estes‡,§

Center for Cell Biology and Cancer Research and Department of Medicine, Albany Medical College, Albany, New York 12208, and Research Service and Medical Service, Stratton VA Medical Center, Albany, New York 12208

Received November 25, 2003; Revised Manuscript Received March 16, 2004

ABSTRACT: Using vertebrate cytoplasmic actin consisting of a mixture of β and γ isoforms, we previously characterized profilin and nucleotide binding to monomeric actin (Kinosian, H. J., et al. (2000) *Biochemistry 39*, 13176−13188) and F-actin barbed end elongation from profilin−actin (PA) (Kinosian, H. J., et al. (2002) *Biochemistry 41*, 6734−6743). Our initial calculations indicated that elongation of F-actin from PA was more energetically favorable than elongation of F-actin from monomeric actin; therefore, the overall actin elongation reaction scheme described by these two linked reactions appeared to be thermodynamically unbalanced. However, we hypothesized that the profilin-induced weakening of MgATP binding by actin reduces the negative free energy change for the formation of profilin−MgATP−actin from MgATP−actin. When this was taken into account, the overall reaction scheme was calculated to be thermodynamically balanced. In our present work, we test this hypothesis by measuring actin filament barbed end elongation of nucleotide-free actin (NF-A) and nucleotide-free profilin−actin (NF-PA). We find that the free energy change for elongation of F-actin by NF-PA is equal to that for elongation of F-actin from NF-A, indicating energetic balance of the linked reactions. In the absence of actin-bound divalent cation, profilin has very little effect on ATP binding to actin; analysis of elongation experiments with divalent cation-free ATP−actin and profilin yielded an approximately energetically balanced reaction scheme. Thus, the data in this present report support our earlier hypothesis.

Profilin is ubiquitous in eukaryotes and has been shown to be essential for development and survival in mice (*1*). Profilin binds to monomeric actin and increases the rate of nucleotide exchange on actin. Profilin binds phophatidyl inositol phosphates and is thus linked to lipid metabolism and the diacylglycerol and Ca^{2+} signaling pathways. Profilin also binds polyproline and proline-rich ligands such as the VASP/Ena/Mena and WASP proteins, linking profilin to cytoskeletal regulation and elongation of actin filaments (*2*). During the process of cell motility-related cytoskeletal reorganization, it is thought that subsequent to rapid cofilin-induced depolymerization of actin filaments, profilin displaces cofilin bound to ADP−actin and causes a rapid exchange of actin-bound nucleotide (*3*). Thus, profilin produces ATP−actin, which is able to polymerize again and charge the actin filament with ATP. Profilin binds to monomeric actin at the "barbed" end between subdomains 1 and 3, leaving the "pointed" end free to associate with an actin filament barbed end; therefore, the profilin−actin complex (PA)[1] can elongate existing actin filaments. In previous work, we characterized nucleotide and profilin binding to monomeric non-muscle vertebrate actin (*4*). In comparison with α skeletal muscle actin (α-SkM-actin), we found that non-muscle β,γ-actin exchanged nucleotide faster and bound profilin with greater affinity. Isothermal denaturation measurements in the absence of nucleotide showed that non-muscle actin was much more stable than α-SkM-actin. Other recent work from our laboratory provided a quantitative and mechanistic analysis of actin filament elongation from profilin−actin using vertebrate non-muscle β,γ-actin and vertebrate profilin (*5*). We found that profilin inhibited elongation of non-muscle β,γ-actin much more than elongation of α-SkM actin. These functional differences between actin isoforms may prove to be significant when modeling actin filament turnover (*3*) or lamellipod extension (*6*).

In the presence of profilin, actin filament barbed end elongation can take place via two pathways, as illustrated in Scheme 1. The first pathway is the simple addition of an actin monomer onto an actin filament barbed end. The second pathway involves three steps: (1) formation of a profilin−actin complex, (2) addition of PA onto the actin filament barbed end, and (3) dissociation of profilin from the actin

† This work was supported by Department of Veterans Affairs Grants 1912-0001 (J.E.E.) and 0398-0002 (L.C.G.).

* To whom correspondence should be addressed at Research Service, Stratton VA Medical Center, 113 Holland Ave., Albany, NY 12208. Phone: (518) 727-7512. Fax: (518) 877-0507. E-mail: hkinosi1@nycap.rr.com.

‡ Center for Cell Biology and Cancer Research, Albany Medical College.

§ Research Service, Stratton VA Medical Center.

|| Department of Medicine, Albany Medical College, and Medical Service, Stratton VA Medical Center.

[1] Abbreviations: PA, profilin−actin complex; NF-A, nucleotide-free actin; NF-PA, nucleotide-free profilin−actin complex; DCF-ATP−actin, divalent cation-free ATP−actin; α-SkM-actin, skeletal muscle α-actin isoform; β,γ-actin, cytoplasmic actin containing a mixture of non-muscle β- and γ-actin isoforms.

10.1021/bi036117s CCC: $27.50
Published on Web 05/01/2004

Scheme 1: Actin Filament Elongation in the Presence of Profilin[a]

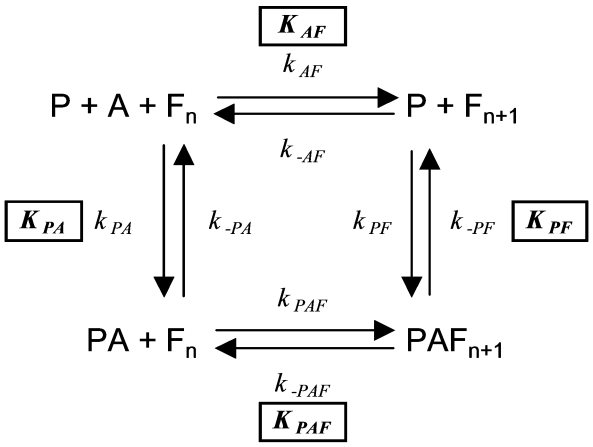

[a] Uppercase *K*'s in boxes indicate equilibrium dissociation constants for each reaction. In the presence of profilin, actin filaments can elongate via two pathways: (1) actin (A) associates with an actin filament (F_n) to produce a filament one subunit in length longer (F_{n+1}), or (2) profilin (P) binds to Actin to form a profilin−actin complex (PA), which associates with an actin filament to produce a filament capped with profilin (PF_{n+1}), and profilin must dissociate from the actin filament end before any subsequent elongation can occur. The ratio of the equilibrium dissociation constants for the two actin filament elongation pathways is $\phi = (K_{AF}K_{PF})/(K_{PA}K_{PAF})$.

filament barbed end. These two pathways are linked such that, to be thermodynamically balanced, the free energy changes for the two actin elongation pathways must be equal. We have previously defined a value of $\phi = (K_{AF}K_{PF})/(K_{PA}K_{PAF}) = 1$ that indicates thermodynamic balance (*5*). Several other laboratories reported variously that the actin filament elongation scheme was either thermodynamically balanced (*7*, *8*) or unbalanced (*9*, *10*). Those reports of thermodynamic imbalance indicated that the negative free energy change was greater for elongation from PA than for elongation from actin alone (i.e., $\phi > 1$). This observation helped to promote the view that the elongation of actin filaments from PA might be coupled to the ATP hydrolysis at the growing actin filament end (*9*, *11*). However, two recent reports contradict that idea. First, actin filament elongation can occur from profilin−MgADP−actin in the absence of ATP (*5*). Second, actin filaments can elongate from profilin−MgATP−actin at rates much faster than the rate of ATP hydrolysis by actin (*12*).

Using Scheme 1, we previously determined for the reactions of profilin, MgATP, monomeric actin, and actin filaments $\phi = 33$, indicating a thermodynamic imbalance (*4*, *5*). To explain this apparent energetic imbalance, we analyzed the formation of the profilin−MgATP−actin complex. The value of the equilibrium dissociation constant for MgATP binding to actin ($K_{AN} = 0.007\ \mu$M) represents a 20-fold greater affinity of MgATP for actin than for profilin−actin ($K_{PAN} = 0.13\ \mu$M) (*4*). Thus, the negative free energy change for the formation of the profilin−MgATP−actin complex calculated from the equilibrium constant, K_{PA} (see Scheme 1), is offset by the positive free energy change for the weakened binding of MgATP by PA compared to the binding by actin alone. Thus, we calculate that the overall profilin−MgATP−actin filament elongation scheme is balanced (within experimental error), with $\phi' = (K_{AF}K_{PF}K_{AN})/(K_{PA}K_{PAF}K_{PAN}) = 1.7$ (*5*).

In the present work, we substantiate our hypothesis that the free energy of nucleotide binding to actin and PA contributes to the energetics of the actin elongation scheme. We show that in the absence of ATP, elongation of nucleotide-free actin (NF-actin) and NF-PA is described by a set of equilibrium constants that result in a thermodynamically balanced energy square. We also show a similar behavior using divalent cation-free ATP−actin (DCF-ATP−actin), analysis of which indicates a value of $\phi = 2$ for the elongation scheme. This is consistent with our previous observation that profilin has relatively little effect on the rate constant for dissociation of ATP from DCF-ATP−actin (*4*).

MATERIALS AND METHODS

Materials. Apyrase, ATP, TRITC−phalloidin, and luciferin/luciferase reagent were from Sigma (St. Louis, MO). *N*-(1-Pyrenyl)iodoacetamide was from Molecular Probes (Eugene, OR).

Protein Preparation. Non-muscle β,γ-actin (*13*) and profilin (*14*) were prepared from bovine spleen. Briefly, clarified bovine spleen homogenate was applied to a 5- × 8-cm poly(L-proline) column, and actin was eluted with buffer containing 0.5 M KI. After the column was washed with 4 M urea, profilin was eluted with 8 M urea. Actin was immediately dialyzed against buffer containing 100 mM KCl and 2 mM $MgCl_2$ to remove KI. F-actin in the eluate was collected by centrifugation, and the pellet was dissolved in and then dialyzed against 2 mM TRIS, pH 8.0, 0.2 mM ATP, 0.2 mM $CaCl_2$, 0.5 mM DTT, 0.01% NaN_3. Profilin was concentrated by application on a CM Sepharose Fast Flow (Pharmacia Biotech, Uppsala, Sweden) column at pH 6.0, eluted with 2 M NaCl, and then dialyzed against 5 mM MOPS, pH 7.2, 0.5 mM DTT. Actin was labeled with *N*-(1-pyrenyl)iodoacetamide as previously described (*15*). Spectrin seeds were prepared from erythrocyte ghosts (*16*, *17*).

Non-muscle β,γ-MgATP−actin was prepared from CaATP−actin by a 1-min incubation with 10 mM MOPS, pH 7.2, 0.5 mM EGTA, 0.25 mM $MgCl_2$, and 0.2 mM ATP. Nucleotide-free non-muscle β,γ-actin was prepared by a modification of the method of De La Cruz and Pollard (*18*). We found that when non-muscle actin was prepared as NF-actin in the presence of 50% sucrose (as per De La Cruz and Pollard), the actin formed polymer (data not shown), making it very difficult to perform the type of elongation experiments needed for our analysis. However, our previous work had determined useful differences between α-SkM-actin and non-muscle β,γ-actin that enabled us to use an alternative method for preparation of nucleotide-free actin. We previously published isothermal denaturation time constants at low ionic strength in the absence of nucleotide (τ_{den}) and found for α-SkM-actin, $\tau_{den} = 5$ s (*19*), and for non-muscle β,γ-actin, $\tau_{den} = 80$ s (*4*), indicating that β,γ-actin is about 16-fold slower to denature than α-SkM-actin under comparable conditions. We also had previously determined (*4*) that non-muscle NF-actin was relatively stable in the presence of 100 mM KCl, with $\tau_{den} = 771 \pm 11$ s, and is further stabilized by profilin binding, with $\tau_{den} = 3273 \pm 239$ s. Under the conditions used here (100 mM KCl, pH 7.0), in the absence of profilin, CaATP dissociates from β,γ-actin with a dissociation time constant of 14 s (unpublished observation), and in the presence of profilin, CaATP dis-

sociation is faster. Here we exploit the relatively fast dissociation of nucleotide from non-muscle actin to rapidly produce NF-actin. The stability of the non-muscle NF-actin species does not allow the formation of a significant amount of denatured actin during the preparation of NF-actin. Non-muscle CaATP−actin was diluted to a final concentration of 1 μM into buffer containing 100 mM KCl, 10 mM MOPS, pH 7.0, 0.5 mM EGTA, 10 U/mL apyrase, and varying profilin concentrations and incubated for 1 min. Apyrase rapidly degrades the ATP and ADP in solution; the absence of ATP was verified using a luciferin/luciferase assay.

Divalent cation-free ATP−actin was produced by diluting CaATP−actin into buffer containing 100 mM KCl, 10 mM MOPS, 2 mM EGTA, 0.5 mM ATP, pH 7.0, and incubating for 1 min.

Actin Polymerization Measurements. Non-muscle β,γ-actin was prepared as MgATP−actin or NF-actin and polymerized by the addition of 100 mM KCl, 2 mM $MgCl_2$, and, as nuclei, either a 20-μL aliquot of phalloidin-stabilized F-actin or a 50-μL aliquot of spectrin seeds. Phalloidin-stabilized actin nuclei were sonicated immediately before use as seeds, producing greater polymerizing activity compared to spectrin seeds. Also, since PA cannot add onto the pointed end of the actin filament, phalloidin F-actin seeds effectively produced only barbed ends capable of elongating from PA. The time constant for phalloidin dissociation from F-actin is long, $\tau = 2000$ s (*20*), compared to the time course of actin polymerization in these experiments, $\tau = 20$ s, so the phalloidin-F-actin seeds are considered stable. The time courses of tryptophan fluorescence (*21*) and light scattering were followed to determine actin polymerization parameters in the absence of profilin. Actin elongation in the presence of profilin was followed by light scattering.

As an additional independent assay of steady-state F-actin concentrations, after actin polymerization was complete, a small aliquot of TRITC−phalloidin (25 nM final concentration) was added to the sample, and the time course of fluorescence intensity increase was recorded and fit by an exponential function (*5*, *20*). This assay corroborated light scattering or tryptophan fluorescence measurements of polymerization. Similar slopes were found for TRITC−phalloidin binding rates versus MgATP−actin control samples compared to those for NF-actin or DCF-ATP−actin, indicating a minimal amount of denaturation for the NF-actin or DCF-ATP−actin polymerization samples (data not shown).

Actin Depolymerization Measurements. Depolymerization rates were measured using 1% pyrene−actin. Actin was polymerized using spectrin seeds as nuclei, and after a polymerization steady-state was reached, varying concentrations of profilin were added to samples of polymerized actin. The free profilin concentrations were calculated using a quadratic binding equation and equilibrium constants for profilin binding to NF-actin, $K_{PA} = 0.013$ μM, and for DCF-ATP−actin, $K_{PA} = 0.037$ μM (*4*). The depolymerization rates were plotted as a function of the free profilin concentration and fit to a hyperbolic function:

$$J = k_{-PAF}\left(\frac{[P]}{[P] + K_{PF}}\right) \quad (1)$$

where J is the depolymerization rate, [P] is the free profilin concentration, and the constants are as defined in Scheme 1.

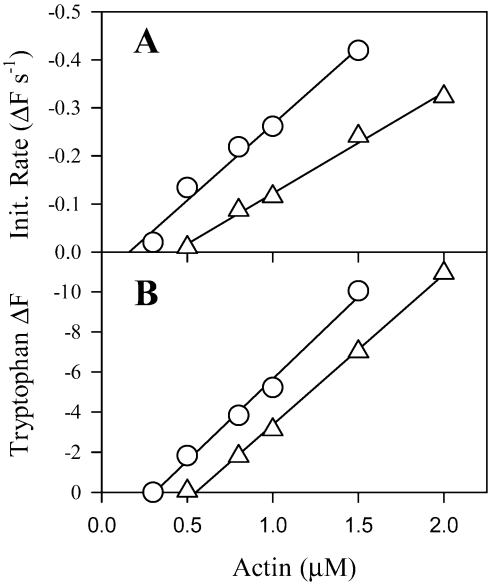

FIGURE 1: Polymerization parameters for non-muscle β,γ-actin. Actin was prepared as either MgATP−actin (○) or nucleotide-free actin (NF-actin) (△) and polymerized by the addition of an aliquot of phalloidin-stabilized F-actin seeds and either 100 mM KCl and 2 mM $MgCl_2$ (MgATP−actin) or 100 mM KCl (NF-actin). The polymerization time courses were followed by tryptophan fluorescence. Panel A shows the initial rates of tryptophan fluorescence intensity change as a function of actin concentration. The slopes of the lines are proportional to the elongation rate constant, k_{AF}, and indicate about a 40% slower polymerization rate constant for NF-actin than for MgATP−actin. Panel B illustrates the change in tryptophan fluorescence intensity of the F-actin samples at steady-state. The data from panels A and B indicate a c_c for MgATP−actin of about 0.2 μM and a c_c for NF-actin of about 0.5 μM.

Alternatively, F-actin was diluted 20-fold into F-buffer containing varying profilin concentrations, and the time course of pyrene fluorescence intensity decrease was measured. Since the total actin concentration is low, the free profilin concentration was considered to be equal to the total profilin concentration. In these experiments, the F-actin depolymerizes at 0 profilin concentration, so the depolymerization rates were fit using

$$J = k_{-AF}\left(1 - \frac{[P]}{[P] + K_{PF}}\right) + k_{-PAF}\left(\frac{[P]}{[P] + K_{PF}}\right) \quad (2)$$

where J is the depolymerization rate, [P] is the free profilin concentration, and the constants are as defined in Scheme 1.

RESULTS

Non-muscle β,γ-Actin Polymerization Rate and Steady-State Measurements. We first analyzed the polymerization characteristics of β,γ-NF-actin in the absence of profilin to determine the appropriate polymerization rate and equilibrium constants. The time courses of nucleated β,γ-actin polymerization were followed using tryptophan fluorescence intensity (*21*). Figure 1 shows the polymerization initial rates and steady-state tryptophan fluorescence intensity changes as a function of actin concentration using MgATP−actin (circles) and NF-actin (triangles). The critical concentration (K_{AF}) for β,γ-MgATP−actin is about 0.2 μM, and that for

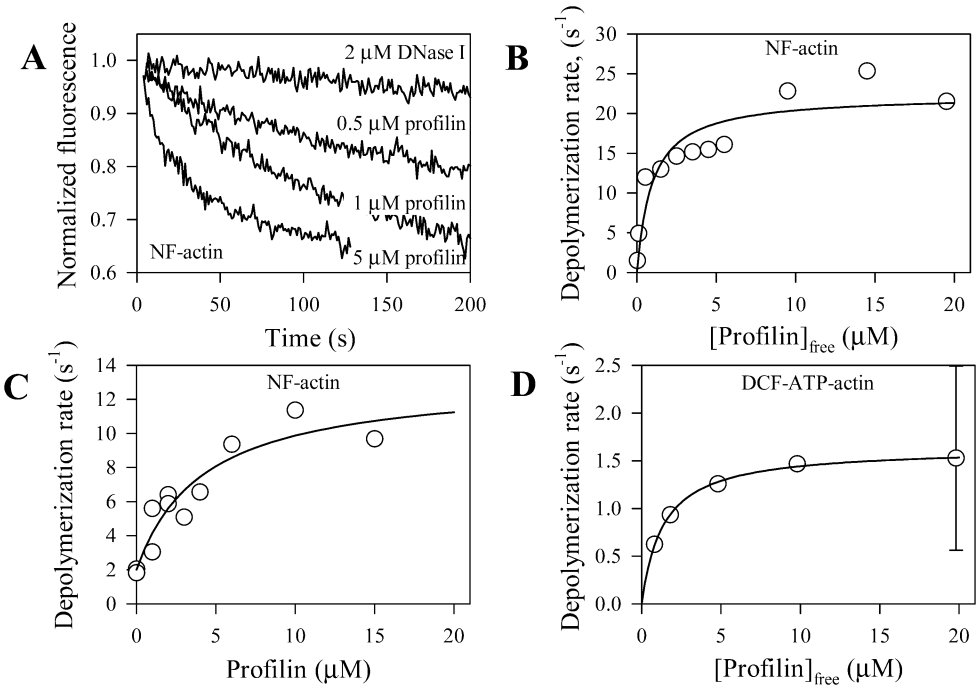

FIGURE 2: Profilin increases the depolymerization rates for non-muscle β,γ-NF-actin. These experiments used F-actin containing 1% pyrene−actin, polymerized with spectrin seeds. (A) 1 μM NF-actin was polymerized, and after steady-state was reached, DNase I or varying concentrations of profilin were added as indicated and the time courses of actin filament depolymerization were recorded. (B) The actin filament depolymerization rates from samples similar to those in panel A were measured and plotted as a function of the free profilin concentration, which was calculated using $K_{PA} = 0.013$ μM and $K_{AF} = 0.5$ μM. A fit using eq 1 yielded $K_{PF} = 1.0 \pm 0.4$ μM. (C) Polymeric NF-actin was diluted 20-fold into buffer containing varying profilin concentrations and 100 mM KCl, 10 mM MOPS, pH 7.0, and 10 U/mL apyrase. The number concentration of actin filament ends was determined from separate elongation assays using MgATP−actin. The initial depolymerization rates are shown as a function of profilin concentration. The line represents a fit to the data using eq 2, yielding $k_{-AF} = 2$ s^{-1}, $k_{-AF} = 13$ s^{-1}, and $K_{PF} = 4.2 \pm 2.2$ μM. (D) In experiments similar to those shown in panel B, 1 μM DCF-ATP−actin was polymerized, and at steady-state varying amounts of profilin were added and the depolymerization rates were determined and plotted as a function of free profilin concentration using $K_{PA} = 0.037$ μM and $K_{AF} = 0.2$ μM. A fit using eq 1 yielded $K_{PF} = 1.3 \pm 1.5$ μM.

β,γ-NF-actin is about 0.5 μM. The K_{AF} for β,γ-MgATP−actin is comparable to that for α-SkM MgATP−actin (*22*, *23*), but the K_{AF} for α-SkM NF-actin has been reported to be 0.06 μM (*24*), much lower than that for β,γ-NF-actin. The slope of the tryptophan fluorescence data (panel A) indicates that the polymerization rate constant is about 40% slower for NF-actin than for MgATP−actin. The absolute value polymerization rate constant for α-SkM MgATP−actin, measured by EM, is 10^7 M^{-1} s^{-1} (*23*) and is the same for β,γ-MgATP−actin (*5*), allowing calculation of the absolute value of the rate constant for β,γ-NF-actin polymerization, $k_{AF} = 6$ μM^{-1} s^{-1}. Similar experiments using DCF-ATP−actin yielded values for the critical concentration $K_{AF} = 0.2$ μM and $k_{AF} = 8$ μM^{-1} s^{-1} (data not shown).

Actin Filament Depolymerization in the Presence of Profilin. The actin depolymerizing activity of profilin is due to its ability to bind to the actin filament barbed end and not due to monomeric actin binding or sequestration (*5*). Figure 2 shows the results from actin depolymerization experiments conducted in two different ways. Panel A shows time course data in which 1 μM NF-actin was polymerized using spectrin seeds, and after steady state was reached, varying amounts of profilin were added to induce depolymerization to a new steady state. The uppermost curve depicts a control experiment in which DNase I was added to depolymerize the actin by acting as an actin monomer sequestering agent that does not affect the actin filament barbed end. Panel B illustrates the initial depolymerization rates for a series of NF-actin depolymerization experiments as a function of the initial free profilin concentration. Free profilin concentration was calculated assuming an actin critical concentration of 0.5 μM and an equilibrium dissociation constant for profilin binding to monomeric actin $K_{PA} = 0.013$ μM (*4*). The data are fit with eq 1, yielding $k_{-PAF} = 25 \pm 3$ s^{-1} and $K_{PF} = 1.0 \pm 0.4$ μM.

We also used an actin filament depolymerization assay in which actin filaments nucleated with spectrin seeds (to create actin filament barbed ends) were diluted into buffer containing varying profilin concentrations. At the beginning of each assay, NF-actin filaments are diluted 20-fold; thus, the actin monomer concentration is about 25 nM and the free profilin concentration is approximately equal to the total profilin concentration. Figure 2C shows the depolymerization rate data and a fit by eq 2, yielding $k_{-AF} = 2.0 \pm 0.8$ s^{-1}, $k_{-PAF} = 13.2 \pm 2.2$ s^{-1}, and $K_{PF} = 4.2 \pm 2.2$ μM. This value of K_{PF} represents a higher affinity for profilin binding to the NF-actin filament barbed end than for profilin binding to the MgATP−actin filament barbed end (*5*).

Data from experiments similar to those shown in Figure 2B, but using DCF-ATP actin, are shown in Figure 2D, and the initial free profilin concentrations were calculated using a value for the critical concentration of 0.2 μM and $K_{PA} = 0.037$ μM (*4*). The fit using eq 1 yields values for DCF-ATP−actin of $k_{-PAF} = 1.6 \pm 0.4$ s^{-1} and $K_{PF} = 1.3 \pm 1.5$ μM.

Modeling the Time Courses for β,γ-NF-Actin Filament Elongation in the Presence of Profilin. We previously published a series of differential equations used to model

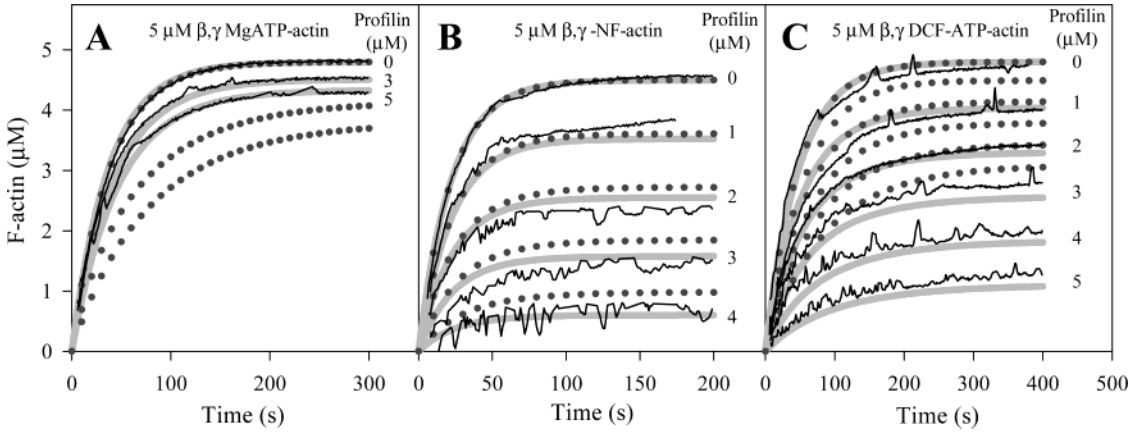

FIGURE 3: Time courses for actin filament elongation from non-muscle β,γ-actin in the presence of profilin. Actin was polymerized in the presence of varying profilin concentrations as indicated, and the polymerization time courses were followed by light scattering. The thin black lines represent the time course data, and the thick gray lines represent a global fit to the data using a series of differential equations derived from Scheme 1 (*5*), using the rate constants listed in Table 1. As a demonstration of the sensitivity of the model to variations of the constants, the dotted gray lines are the time courses predicted using alternate values for K_{PAF} that results in $\phi = 10$ (see text for details). (A) As a control, MgATP−actin was used for elongation, and the data were fit by a series of constants resulting in a value of $\phi = 20$. (B) NF-actin elongation time courses and fit by the model using constants resulting in a value of $\phi = 1$, indicating thermodynamic balance of the reaction scheme. (C) DCF-ATP−actin elongation time courses and fit by the model using constants resulting in a value of $\phi = 2$, indicating approximate thermodynamic balance of the reaction.

the time course of actin filament elongation in the presence of profilin (*5*). Rate constants for profilin binding to monomeric MgATP−actin, DCF-ATP−actin, and NF-actin have been previously published (*4*). In the present report we have determined the values for the rate constants for β,γ-NF-actin polymerization, $k_{AF} = 6\ \mu M^{-1}\ s^{-1}$ and $k_{-AF} = 3\ s^{-1}$ (Figures 1 and 2), which are consistent with the K_{AF} (critical concentration) value of 0.5 μM for β,γ-NF-actin (Figure 1). We were not able to measure the rate constants for association (k_{PF}) or dissociation (k_{-PF}) of NF-PA with the actin filament barbed end. However, simulations using a constant value for K_{PF} of ~2 μM (from data in Figure 2), and varying the value of k_{PF} from 0.01 to 1000 $\mu M^{-1}\ s^{-1}$ and varying k_{-PF} inversely, showed no noticeable effect on the predicted time courses for actin filament elongation. To choose a pair of rate constants for our simulations, we made the assumption that k_{PF} is equal to the rate constant for profilin binding to monomeric β,γ-NF-actin, $k_{PA} = 11\ \mu M^{-1}\ s^{-1}$ (*4*); thus, $k_{-PF} = K_{PF}k_{PF} = 2\ \mu M \times 11\ \mu M^{-1}\ s^{-1} = 22\ s^{-1}$. From actin filament depolymerization experiments (Figure 2C), we have determined the rate constant for dissociation of NF-PA from the actin filament barbed end, $k_{-PAF} = 13\ s^{-1}$. Using the constants discussed above, we then need only to determine the rate constant for association of NF-PA with the actin filament barbed end, k_{PAF}, to completely describe the time course of actin filament elongation and to calculate the free energy changes for the energy square. The relatively poor polymerization of complexes of NF-actin and DCF-ATP−actin with profilin has prevented us from directly determining the association rate constant, k_{PAF}, or the equilibrium constant, K_{PAF}, using these actin species. Therefore, the value for k_{PAF} was determined from a global fit to β,γ-NF-actin filament elongation time course data using a series of differential equations (*5*) and the rate constants described above. All the constants used for the actin filament elongation time course simulations are listed in Table 1.

Table 1: Equilibrium Constants Used for Actin Filament Elongation Modeling[a]

	actin		
	MgATP	NF	DCF-ATP
ϕ[b]	20	1	2
K_{AF} (μM)	0.2	0.5	0.2
k_{AF} ($\mu M^{-1}\ s^{-1}$)	10	6	8
k_{-AF} (s^{-1})	2	3	1.6
K_{PA} (μM)	0.1[c]	0.013[c]	0.037[c]
k_{PA} ($\mu M^{-1}\ s^{-1}$)	15[c]	11[c]	15[c]
k_{-PA} (s^{-1})	1.5[c]	0.14[c]	0.55[c]
K_{PAF} (μM)	2[d]	80	5
k_{PAF} ($\mu M^{-1}\ s^{-1}$)	9[d]	0.16	2
k_{-PAF} (s^{-1})	20[d]	13	10
K_{PF} (μM)	20[d]	2	2
k_{PF} ($\mu M^{-1}\ s^{-1}$)	15[d]	11	15
k_{-PF} (s^{-1})	300[d]	22	30

[a] These constants are defined in Scheme 1, and the values listed were used to model the actin filament elongation time courses shown in Figure 3. [b] $\phi = (K_{AF}K_{PF})/(K_{PA}K_{PAF})$. [c] Determined in ref *4*. [d] Determined in ref *5*.

Figure 3 shows time course data (thin black lines) and fit (wide gray lines) for elongation of 5 μM MgATP−actin (panel A), 5 μM NF-actin (panel B), and 5 μM DCF-ATP−actin (panel C) in the presence of varying concentrations of profilin as indicated on the figures. The rate and equilibrium constants used for simulation of the MgATP−actin time courses are similar to those previously published (*5*). For NF-actin (panel B), a value for $k_{PAF} = 0.16\ \mu M^{-1}\ s^{-1}$ was derived from the fit. We can therefore calculate the equilibrium constant for NF-PA binding to the β,γ-NF-actin filament barbed end: $K_{PAF} = k_{-PAF}/k_{PAF} = 13\ s^{-1}/0.16\ \mu M^{-1}\ s^{-1} = 80\ \mu M$. Panel C shows the time course data for DCF-ATP−actin which are well described using a value for $k_{PAF} = 2\ \mu M^{-1}s^{-1}$ and $K_{PAF} = k_{-PAF}/k_{PAF} = 10\ s^{-1}/2\ \mu M^{-1}\ s^{-1} = 5\ \mu M$. The rate constants used for DCF-ATP−actin were determined by the same means as described for NF-actin, employing previously published values for profilin binding to monomeric actin (*4*), data from polymerization experiments to determine actin polymerization constants (not shown), and actin depolymerization experiments in the presence of profilin to determine profilin binding to F-actin (Figure 2D).

Elongation of NF-Actin in the Presence of Profilin Is Energetically Balanced. Among the equilibrium constants necessary for determining the thermodynamic balance of Scheme 1, values for K_{PA} have been previously determined in our laboratory (*4*), and values for the actin critical concentration, K_{AF}, have been determined and/or confirmed in the present report. The value for the equilibrium dissociation constant for profilin binding to the actin filament barbed end, K_{PF}, is estimated from the increased actin filament depolymerization rates in the presence of profilin (Figure 3). The direct determination of the equilibrium dissociation constant for PA binding to the actin filament barbed end has proven to be problematic, but by estimating the value for k_{PAF} using a model of the time courses for actin filament elongation in the presence of profilin, the value for K_{PAF} was determined indirectly by calculation from k_{-PAF}/k_{PAF}. Varying values for k_{-PAF} and k_{PAF} indicate that the fit to the time course data appears to be less dependent on the rate constants than on the equilibrium constant. The constants used to model the data in Figure 3 are listed in Table 1, and from these constants we calculate the value of $\phi = (K_{AF}K_{PF})/(K_{PA}K_{PAF})$ to evaluate the thermodynamic balance of the reaction scheme. For MgATP−actin (Figure 3A), we calculate $\phi = 20$, indicating an apparent thermodynamic imbalance, as previously reported (*5*). However, for NF-actin we calculate $\phi = 1$, indicating a thermodynamic balance for the reaction scheme, supporting the hypothesis that the difference in the energy of MgATP binding to actin and profilin−actin contributes to the overall free energy change for the reaction scheme. Moreover, the results for DCF-ATP−actin allow calculation of $\phi = 2$, again indicating a thermodynamically balanced reaction scheme, within experimental error. The results for DCF-ATP−actin are consistent with the observation that profilin binding to DCF-ATP−actin increases the ATP dissociation rate from actin by only about 50% as compared to a weakening of 25-fold for MgATP−actin (*4*).

As an estimation of error and robustness of the model, in addition to the fits of the model (solid gray lines) to the data in Figure 3, the dotted lines illustrate the actin elongation time courses predicted using constants that result in a value of $\phi = 10$. All other constants were unchanged, except that the value of k_{-PAF} was adjusted to yield K_{PAF} values that resulted in $\phi = 10$ for each type of actin. In Figure 3A, for MgATP−actin, changing the K_{PAF} so that the value of ϕ goes to 10 from 20 results in an obvious change in the predicted time courses. This indicates that the model is relatively sensitive to that parameter and is fairly robust for evaluating the goodness of fit to the data. For NF-actin (Figure 3B), changing K_{PAF} 10-fold and thereby changing ϕ to 10 from 1 results in a relatively small effect on the predicted time courses for actin filament elongation. In this case, the model is not robust when evaluating the goodness of fit for that parameter. Although a set of constants that result in a thermodynamically balanced reaction scheme for NF-actin elongation are entirely consistent with the time course data, an alternative set of constants that indicate energetic imbalance could also fit the data. However, the results for DCF-ATP−actin (Figure 3C) show that a 5-fold change in K_{PAF}, so that $\phi = 10$ compared to $\phi = 2$, results in an obvious change in the predicted actin elongation time courses, and thus indicates a greater certainty for the constants used for the DCF-ATP−actin data than for NF-actin data.

DISCUSSION

In our previous work (*5*), we found that the elongation of actin filaments from MgATP−actin and MgADP−actin in the presence of profilin appeared to be energetically unbalanced when they were analyzed without considering nucleotide binding to actin and PA. Since profilin binding to actin weakens actin's affinity for MgATP or MgADP, we hypothesized that this weaker nucleotide binding to PA could contribute to the overall free energy change calculated for the actin filament elongation reaction. In the present work we have prepared non-muscle β,γ-actin without a bound nucleotide in order to analyze the overall reaction scheme without the complicating factor of the effect of profilin on the nucleotide binding by actin. We find that a thermodynamically balanced reaction scheme in the absence of nucleotide is consistent with the experimental data. Moreover, analysis of Scheme 1 using actin containing bound ATP but no Mg^{2+} also indicates an energetically balanced scheme. This is consistent with our hypothesis because profilin only slightly affects ATP binding to DCF-actin (*4*). The data in the present report support our hypothesis that calculation of the free energy change for profilin binding to monomeric actin must include the binding of nucleotide to actin in the ternary profilin−nucleotide−actin complex (*5*).

Comparison of NF-Actin and MgATP-Actin. We previously reported that profilin binds to monomeric β,γ-NF-actin with nearly 10-fold higher affinity ($K_{PA} = 0.013$ μM) than to monomeric β,γ-MgATP−actin ($K_{PA} = 0.1$ μM) (*4*). This relative binding affinity appears to hold true for profilin binding to the actin filament barbed end; we find that profilin binds more tightly to the NF-actin filament barbed ends, with an equilibrium constant $K_{PF} = 2$ μM, compared to that for MgATP−actin, $K_{PF} = 20$ μM. We also reported that the affinity of profilin for the actin filament barbed end is 200-fold weaker than that for monomeric MgATP−actin and now find a comparable affinity change of approximately 200-fold for NF-actin. These observations suggest that profilin−MgATP−actin and profilin−NF-actin elongate actin filaments by same mechanism. Although actin filaments elongate from profilin−MgATP−actin at nearly the same rate as from MgATP−actin (*5*), profilin−NF-actin appears to have a much reduced elongation rate constant, $k_{PAF} = 0.16$ μM^{-1} s^{-1} compared to that of NF-actin alone, $k_{AF} = 6$ μM^{-1} s^{-1}.

In our previous work (*5*), we suggested that when PA associates with an actin filament barbed end, the new intermolecular bonds that are formed pull the actin monomer into a conformation that releases profilin. In the case of profilin−MgATP−actin, this process appears to be very efficient; the association rate constant for PA is equal to that for actin alone. In contrast, for profilin−NF-actin, the process appears to be inefficient; the association rate constant for NF-PA is very much less than that for NF-actin alone. It appears that when NF-PA associates with an actin filament barbed end, it is more likely to dissociate as the NF-PA complex than for profilin to dissociate from the actin. This interpretation is consonant with the observation that profilin binds with greater affinity to monomeric NF-actin than to monomeric MgATP−actin (*4*). In addition to profilin, other ligands of actin have been shown to reduce the association rate constant for actin polymerization. For example, the elongation rate constant, k_{AF}, for MgATP−actin is $\sim 10^7$ M^{-1}

s^{-1} (*23*); in comparison, for CaATP−actin k_{AF} is about one-half of that value, and for MgADP−actin, $k_{AF} \approx 10^6$ M^{-1} s^{-1} (*22*), about an order of magnitude slower than that for MgATP−actin (*23*).

Effect of the Bound Nucleotide on PA Elongation. Our data support the idea that when actin is complexed with profilin, the bound nucleotide of actin bridges the two major actin domains and helps to hold the actin molecule in a conformation that is most able to polymerize. Our previous work (*4*) showed that profilin and nucleotide binding to actin have antagonistic effects; profilin binds more weakly to actin containing bound MgATP, which binds to actin with very high affinity, and profilin binds more strongly to actin containing no bound nucleotide. Thus, the actin-bound nucleotide appears to hold the actin in a conformation that is less suitable for profilin binding. We also found that profilin binding to the monomeric actin shifts the actin conformation toward a more open central cleft (as shown in the crystal structure of profilin−actin by Chik et al. (*25*)) that weakens nucleotide binding to actin. In the absence of MgATP bound to actin, profilin binds more tightly to the NF-actin monomer and appears to shift the actin conformation to one in which the NF-PA is much less able to polymerize. Adding ATP to NF-PA enhances the ability of the profilin−NF-actin complex to maintain a polymerizable conformation, and adding Mg^{2+} to the complex of profilin and DCF-ATP−actin further enables PA to achieve the polymerizable conformation of MgATP−actin alone.

Comparison of Kinetic and Structural Data. Recent crystallographic structures of uncomplexed actin containing either bound ATP or ADP have indicated that the ATP hydrolysis by actin results in a conformational change in actin subdomain 2, in which a flexible loop in ATP−actin becomes a helix in ADP−actin (*26*, *27*). The crystal structures of both ATP−actin and ADP−actin are in the "closed" configuration, in which the two major actin domains on either side of the central nucleotide-binding cleft of actin are in close contact with each other. These authors argue that NF-actin would exist in the "open" state.

Proteins exist in a distribution of various conformational states, with the occupancy of any particular conformation determined by the free energy of that state. The transition between the actin "open" state and the "closed" state observed for crystals of actin complexed with profilin can be made with very little free energy change (*25*). We suggest that the bound nucleotide restricts the conformational freedom of actin. From the numerous crystal structures of actin, it appears that in the "closed" state the actin-bound nucleotide is sterically blocked from dissociation; thus, the conformational switch to the "open" state is required for nucleotide dissociation from actin or for nucleotide association with actin. Since nucleotides can associate only to NF-actin (i.e., the actin nucleotide binding cleft is empty), this implies that NF-actin must exist in the "open" conformation, at least transiently. We previously measured rate constants for nucleotide association with actin to be about 10^6 M^{-1} s^{-1} (*4*, *12*), which is slower than expected for a diffusion-limited reaction of a small molecule with a protein, suggesting that NF-actin is only transiently in the "open" conformation, or that other orientation or charge effects impede association of nucleotides to actin.

Even though both MgATP and MgADP bind to actin in the central cleft and stabilize the actin conformation compared to NF-actin, the two nucleotides have opposite effects on actin polymerization. Here we observe that NF-actin polymerizes less well than MgATP−actin but better than MgADP−actin: the critical concentrations for non-muscle MgATP−actin, NF-actin, and MgADP−actin are 0.2, 0.5, and 1.7 μM, respectively. Thus, the removal of the γ phosphate group from actin-bound ATP per se is not what regulates the actin polymerization function. This points to the idea that bound MgADP promotes a particular actin conformation, perhaps involving subdomain 2 (*26*, *27*), that inhibits actin polymerization and promotes actin filament depolymerization.

Interestingly, the actin conformational equilibria may be quite different in F-actin. One report (*28*) indicates that the ATP hydrolysis by actin in the filament results in a shift of the "closed" ATP−actin conformation to an "open" ADP−actin conformation. EM reconstructions of NF-actin filaments indicate that the monomers in the filament appear to be in a closed conformation and maintain strong contacts along the long-pitch helical strands (*24*). Moreover, the inaccessibility of ATP to the nucleotide binding site in the actin filament is most likely due to a closed actin cleft.

Profilin Function in Vivo. These observations suggest that in vivo, profilin may be very efficacious in allowing only MgATP−actin to polymerize, thus forming actin filaments charged with ATP and ADP−P_i. In this way, the lifetime of the actin filaments can be regulated by the dissociation of P_i and the "phosphate clock" which controls binding of cofilin, debranching, and depolymerization of actin filaments (*2*).

REFERENCES

1. Witke, W., Sutherland, J. D., Sharpe, A., Arai, M., and Kwiatkowski, D. J. (2001) Profilin I is essential for cell survival and cell division in early mouse development, *Proc. Natl. Acad. Sci. U.S.A. 98*, 3832−3836.
2. Pollard, T. D., Blanchoin, L., and Mullins, R. D. (2000) Molecular mechanisms controlling actin filament dynamics in nonmuscle cells, *Annu. Rev. Biophys. Biomol. Struct. 29*, 545−576.
3. Didry, D., Carlier, M. F., and Pantaloni, D. (1998) Synergy between actin depolymerizing factor/cofilin and profilin in increasing actin filament turnover, *J. Biol. Chem. 273*, 25602−25611.
4. Kinosian, H. J., Selden, L. A., Gershman, L. C., and Estes, J. E. (2000) Interdependence of profilin, cation, and nucleotide binding to vertebrate non-muscle actin, *Biochemistry 39*, 13176−13188.
5. Kinosian, H. J., Selden, L. A., Gershman, L. C., and Estes, J. E. (2002) Actin Filament Barbed End Elongation with Non-Muscle MgATP−Actin and MgADP−Actin in the Presence of Profilin, *Biochemistry 41*, 6734−6743.
6. Mogilner, A., and Edelstein-Keshet, L. (2002) Regulation of actin dynamics in rapidly moving cells: a quantitative analysis, *Biophys. J. 83*, 1237−1258.
7. Pring, M., Weber, A., and Bubb, M. R. (1992) Profilin−actin complexes directly elongate actin filaments at the barbed end, *Biochemistry 31*, 1827−1836.
8. Kang, F., Purich, D. L., and Southwick, F. S. (1999) Profilin promotes barbed-end actin filament assembly without lowering the critical concentration, *J. Biol. Chem. 274*, 36963−36972.
9. Pantaloni, D., and Carlier, M. F. (1993) How profilin promotes actin filament assembly in the presence of thymosin beta 4, *Cell 75*, 1007−1014.
10. Pollard, T. D., and Cooper, J. A. (1984) Quantitative analysis of the effect of Acanthamoeba profilin on actin filament nucleation and elongation, *Biochemistry 23*, 6631−6641.

11. Perelroizen, I., Didry, D., Christensen, H., Chua, N. H., and Carlier, M. F. (1996) Role of nucleotide exchange and hydrolysis in the function of profilin in actin assembly, *J. Biol. Chem. 271*, 12302−12309.
12. Blanchoin, L., and Pollard, T. D. (2002) Hydrolysis of ATP by polymerized actin depends on the bound divalent cation but not profilin, *Biochemistry 41*, 597−602.
13. Selden, L. A., Kinosian, H. J., Estes, J. E., and Gershman, L. C. (2000) Cross-linked dimers with nucleating activity in actin prepared from muscle acetone powder, *Biochemistry 39*, 64−74.
14. Selden, L. A., Kinosian, H. J., Estes, J. E., and Gershman, L. C. (1999) Impact of profilin on actin-bound nucleotide exchange and actin polymerization dynamics, *Biochemistry 38*, 2769−2778.
15. Kouyama, T., and Mihashi, K. (1981) Fluorometry study of N-(1-pyrenyl) iodoacetamide-labeled F-actin. Local structural change of actin protomer both on polymerization and on binding of heavy meromyosin, *Eur. J. Biochem. 114*, 33−36.
16. Lin, D. C., and Lin, S. (1978) High affinity binding of [3H]-dihydrocytochalasin B to peripheral membrane proteins related to the control of cell shape in the human red cell, *J. Biol. Chem. 253*, 1415−1419.
17. Casella, J. F., Maack, D. J., and Lin, S. (1986) Purification and initial characterization of a protein from skeletal muscle that caps the barbed ends of actin filaments, *J. Biol. Chem. 261*, 10915−10921.
18. De La Cruz, E. M., and Pollard, T. D. (1995) Nucleotide-free actin: stabilization by sucrose and nucleotide binding kinetics, *Biochemistry 34*, 5452−5461.
19. Kinosian, H. J., Selden, L. A., Estes, J. E., and Gershman, L. C. (1993) Nucleotide binding to actin. Cation dependence of nucleotide dissociation and exchange rates, *J. Biol. Chem. 268*, 8683−8691.
20. De La Cruz, E., and Pollard, T. D. (1994) Transient kinetic analysis of rhodamine phalloidin binding to actin filaments, *Biochemistry 33*, 14387−14392.
21. Selden, L. A., Kinosian, H. J., Estes, J. E., and Gershman, L. C. (1994) Influence of the high affinity divalent cation on actin tryptophan fluorescence, *Adv. Exp. Med. Biol. 358*, 51−57.
22. Selden, L. A., Gershman, L. C., and Estes, J. E. (1986) A kinetic comparison between Mg-actin and Ca-actin, *J. Muscle Res. Cell Motil. 7*, 215−224.
23. Pollard, T. D. (1986) Rate constants for the reactions of ATP- and ADP-actin with the ends of actin filaments, *J. Cell Biol. 103*, 2747−2754.
24. De La Cruz, E. M., Mandinova, A., Steinmetz, M. O., Stoffler, D., Aebi, U., and Pollard, T. D. (2000) Polymerization and structure of nucleotide-free actin filaments, *J. Mol. Biol. 295*, 517−526.
25. Chik, J. K., Lindberg, U., and Schutt, C. E. (1996) The structure of an open state of β-actin at 2.65 Å resolution, *J. Mol. Biol. 263*, 607−623.
26. Otterbein, L. R., Graceffa, P., and Dominguez, R. (2001) The crystal structure of uncomplexed actin in the ADP state, *Science 293*, 708−711.
27. Graceffa, P., and Dominguez, R. (2003) Crystal Structure of Monomeric Actin in the ATP State. Structural Basis of Nucleotide-Dependent Actin Dynamics, *J. Biol. Chem. 278*, 34172−34180.
28. Belmont, L. D., Orlova, A., Drubin, D. G., and Egelman, E. H. (1999) A change in actin conformation associated with filament instability after Pi release, *Proc. Natl. Acad. Sci. U.S.A. 96*, 29−34.

BI036117S